(12) INTERNATIONAL APPLICATION PUBLISHED UNDER THE PATENT COOPERATION TREATY (PCT)

(19) World Intellectual Property Organization
International Bureau

(10) International Publication Number
WO 2014/146017 A1

(43) International Publication Date
18 September 2014 (18.09.2014)

(51) International Patent Classification:
H01B 12/02 (2006.01) *H01B 1/04* (2006.01)

(21) International Application Number:
PCT/US2014/030887

(22) International Filing Date:
17 March 2014 (17.03.2014)

(25) Filing Language: English

(26) Publication Language: English

(30) Priority Data:
61/792,496 15 March 2013 (15.03.2013) US

(71) Applicant: UNIVERSITY OF UTAH RESEARCH FOUNDATION [US/US]; 615 Arapeen Drive, Suite 310, Salt Lake City, UT 84108 (US).

(72) Inventors; and
(71) Applicants : LIU, Feng [US/US]; 8028 Madsen Court, Sandy, UT 84093 (US). LIU, Zheng [CN/US]; 1050 Markea Avenue, Salt Lake City, UT 84102 (US). SI, Chen [CN/US]; Department of Physics, Tsinghua U., Tsinghua University, Beijing, 100084 (CN).

(74) Agent: LOVEJOY, Brett, A.; Morgan, Lewis & Bockius LLP, One Market, Spear Street Tower, San Francisco, CA 94105 (US).

(81) Designated States *(unless otherwise indicated, for every kind of national protection available)*: AE, AG, AL, AM, AO, AT, AU, AZ, BA, BB, BG, BH, BN, BR, BW, BY, BZ, CA, CH, CL, CN, CO, CR, CU, CZ, DE, DK, DM, DO, DZ, EC, EE, EG, ES, FI, GB, GD, GE, GH, GM, GT, HN, HR, HU, ID, IL, IN, IR, IS, JP, KE, KG, KN, KP, KR, KZ, LA, LC, LK, LR, LS, LT, LU, LY, MA, MD, ME, MG, MK, MN, MW, MX, MY, MZ, NA, NG, NI, NO, NZ, OM, PA, PE, PG, PH, PL, PT, QA, RO, RS, RU, RW, SA, SC, SD, SE, SG, SK, SL, SM, ST, SV, SY, TH, TJ, TM, TN, TR, TT, TZ, UA, UG, US, UZ, VC, VN, ZA, ZM, ZW.

(84) Designated States *(unless otherwise indicated, for every kind of regional protection available)*: ARIPO (BW, GH, GM, KE, LR, LS, MW, MZ, NA, RW, SD, SL, SZ, TZ, UG, ZM, ZW), Eurasian (AM, AZ, BY, KG, KZ, RU, TJ, TM), European (AL, AT, BE, BG, CH, CY, CZ, DE, DK, EE, ES, FI, FR, GB, GR, HR, HU, IE, IS, IT, LT, LU, LV, MC, MK, MT, NL, NO, PL, PT, RO, RS, SE, SI, SK, SM, TR), OAPI (BF, BJ, CF, CG, CI, CM, GA, GN, GQ, GW, KM, ML, MR, NE, SN, TD, TG).

Declarations under Rule 4.17:
— *as to applicant's entitlement to apply for and be granted a patent (Rule 4.17(ii))*
— *as to the applicant's entitlement to claim the priority of the earlier application (Rule 4.17(iii))*

Published:
— *with international search report (Art. 21(3))*

[Continued on next page]

(54) Title: GRAPHENE-BASED SUPERCONDUCTORS

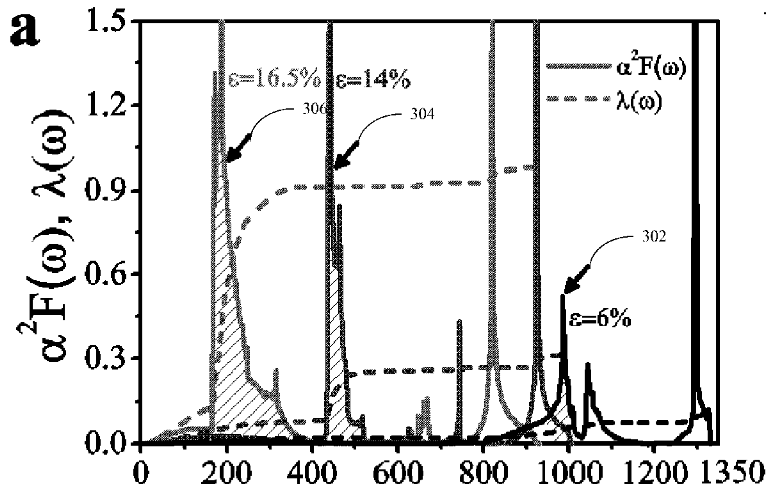

Figure 3(a)

(57) Abstract: The disclosed implementations include graphene-based superconductors and methods of producing graphene based superconductors. In particular, in contrast to the inherent electrical characteristics of graphene, in accordance with various implementations graphene is converted to a BCS superconductor, having a critical temperature substantially above zero Kelvin (K), using a combination of charge doping and tensile strain. Charge doping enables enlargement of the Fermi surface of graphene, and tensile strain enables an increase in electron-phonon coupling. For example, a critical temperature T_c of 30 K can be achieved by a combination of a doping level of ~3.5×10^{14} cm^{-2} and a strain level of ~16%. In some implementations, a critical temperature T_c of 30 K makes graphene-based superconductors commercially viable for a number of industrial applications.

WO 2014/146017 A1

— *before the expiration of the time limit for amending the claims and to be republished in the event of receipt of amendments (Rule 48.2(h))*

Graphene-Based Superconductors

CROSS REFERENCE TO RELATED PATENT APPLICATION

[0001] This application claims priority to United States Provisional Patent Application No. 61/792,496, entitled "Graphene-Based Superconductors," filed March 15, 2013, which is hereby incorporated by reference in its entirety.

TECHNICAL FIELD

[0002] The disclosed implementations relate to superconductors, and in particular, to graphene-based superconductors and methods of producing graphene-based superconductors.

BACKGROUND

[0003] Pure (e.g., intrinsic) graphene has a number of distinguishing properties. For example, electrically, intrinsic graphene has the highest carrier mobility of known materials with massless Dirac Fermions. Optically, intrinsic graphene has the largest adsorption per atomic layer in the visible range of known materials. And mechanically, intrinsic graphene is generally considered the strongest two dimensional (2D) material known in nature.

[0004] However, intrinsic graphene cannot be used as a conventional Bardeen-Cooper-Schrieffer (BCS) superconductor at a critical temperature T_c of more than a few degrees Kelvin (K) because intrinsic graphene exhibits very weak electron-phonon coupling (EPC). Two inherent electro-chemical characteristics of intrinsic graphene cause the very weak EPC. First, intrinsic graphene has a point-like Fermi surface (Dirac point) with a vanishing density of states (DOS). Second, intrinsic graphene has a weak electron-phonon pairing potential (V_{ep}).

[0005] Charge doping can be used to enlarge the Fermi surface of graphene. However, charge doping alone cannot make graphene a BCS superconductor because the electron-phonon pairing potential V_{ep} for graphene (which is independent of the doping level) is small, and because it is not possible to dope at a high enough level to overcome the small V_{ep} of graphene using other mechanisms to raise the EPC. Moreover, using known methods and technology, it is not possible to change the weak electron-phonon pairing potential V_{ep} of graphene.

SUMMARY

[0006] Various implementations of systems, methods and devices within the scope of the appended claims each have several aspects, no single one of which is solely responsible for the desirable attributes described herein. Without limiting the scope of the appended claims, some prominent features are described herein. After considering this discussion, and particularly after reading the section entitled “Detailed Description” one will understand how the features of various implementations comprise graphene-based superconductors and methods of producing graphene-based superconductors.

[0007] One aspect of the disclosure is graphene-based superconductive device. In some implementations, graphene-based superconductive device includes a stack of charge doped graphene characterized by a doping level within a threshold doping range, a force transference structure that engages respective at least two portions of the stack of charge doped graphene. The force transference structure is provided to transfer a force into the stack of charge doped graphene thereby causing tensile strain in the stack of charge doped graphene. The tensile strain is characterized by a strain level within a threshold strain range. The combination of the doping level and strain level determine the critical temperature of the stack of charge doped graphene.

[0008] Another aspect of the disclosure is a method of producing a graphene-based superconductive device. In some implementations, the method includes providing a stack of charge doped graphene characterized by a doping level within a threshold doping range, and imparting a force to the stack of charge doped graphene to produce tensile strain in the stack of charge doped graphene. This tensile strain is characterized by a strain level within a threshold strain range. The combination of the doping level and the strain level determine the critical temperature of the stack of charge doped graphene.

BRIEF DESCRIPTION OF THE DRAWINGS

[0009] So that the present disclosure can be understood in greater detail, a more particular description may be had by reference to the aspects of various implementations, some of which are illustrated in the appended drawings. The appended drawings, however, merely illustrate the more pertinent aspects of the present disclosure and are therefore not to be considered limiting, for the description may admit to other effective aspects.

[0010] Figures 1(a) and 1(b) are graphs showing the density of states and electron-phonon coupling strength. In particular, in Figure 1(a), the N(0) and λ of p-type graphene under different doping levels is illustrates. In the insert to Figure 1(a), V_{ep} versus doping level for unstrained graphene is illustrated. In Figure 1(b), V_{eV} under different biaxial strains (σ) for 3% p-doped graphene is illustrated.

[0011] Figures 2(a) and 2(b) are three-dimensional graphs showing the relationship between tensile strain, hole doping and the critical temperature of charge-doped graphene. In particular, Figure 2(a) is a three-dimensional plot of $\lambda(n,\varepsilon)$ and Figure 2(b) is a three-dimensional plot of $T_c(n,\varepsilon)$.

[0012] Figure 3(a)-3(f) are graphs showing Eliashberg functions for charge-doped graphene. In particular, the Eliashberg functions for 1%(a), 2%(c) and 3%(e) hole doped graphene under 6% (line 302), 14% (line 304) and 16.5% (line 306), (b), (d) and (f), $\langle\omega^2\rangle^{1/2}$ under different tensile strain (ε) for 1%, 2% and 3% hole doped graphene, respectively, with Insets showing λ versus $\langle\omega^2\rangle^{-2}$.

[0013] Figure 4 is a graph of logarithmically averaged phonon frequency as a function of tensile strain in charge-doped graphene.

[0014] Figure 5 is a perspective view of a graphene-based superconductive device in accordance with some implementations, in which there is a first step in which a charge-doped graphene stack is arranged in between two hollow plates and a second step in which the graphene is stretched using an arcuate member.

[0015] In accordance with common practice the various features illustrated in the drawings may not be drawn to scale. Accordingly, the dimensions of the various features may be arbitrarily expanded or reduced for clarity. In addition, some of the drawings may not depict all of the components of a given system, method or device. Finally, like reference numerals may be used to denote like features throughout the specification and figures.

DETAILED DESCRIPTION

[0016] The disclosed implementations include graphene-based superconductors and methods of producing graphene based superconductors. In particular, in contrast to the inherent electrical characteristics of graphene, in accordance with various implementations graphene is

converted to a BCS superconductor having a critical temperature substantially above zero Kelvin (K) using a combination of charge doping and tensile strain. Charge doping enables enlargement of the Fermi surface of graphene, and tensile strain enables an increase in electron-phonon coupling. For example, a critical temperature T_c of 30 K can be achieved by a combination of a doping level of $\sim 3.5\times 10^{14}$ cm^{-2} and a strain level of ~16%, which is the highest known critical temperature for a single-element material above the temperature of liquid hydrogen. In some implementations, a critical temperature T_c of 30 K makes graphene-based superconductors commercially viable for a number of industrial applications.

[0017] Numerous details are described herein in order to provide a thorough understanding of the example implementations illustrated in the accompanying drawings. However, the invention may be practiced without many of the specific details and is only limited by the language of the claims. Well-known methods, components, and circuits have not been described in exhaustive detail so as not to unnecessarily obscure more pertinent aspects of the implementations described herein.

[0018] In some implementations, graphite-based structures, *e.g.* graphene quantum dots, graphene nanoribbons (GNRs), graphene nanonetworks, graphene plasmonics and graphene super-lattices, exhibit many exceptional chemical, mechanical, electronic and optical properties, and are very desirable for use in electronic devices, composite materials, and energy generation and storage. Such graphite-based structures in general comprise a graphene layer, typically nanometers thick and having a characteristic dimension also in the nanometers range. For example, in order to obtain adequate band gaps for operation at room temperature, GNRs are required to have a width within a few nanometers due to the inverse relationship between the band gap and the width of the GNRs.

[0019] In some implementations, various methods are provided for fabricating graphite-based structures while achieving desired size, specified geometries, and characterized electronic properties of the graphite-based structures. These methods include, but are not limited to, (1) the combination of e-beam lithography and oxygen plasma etching; (2) stripping of graphite that is sonochemically processed; and (3) bottom-up chemical synthesis, *e.g.*, by cyclodehydrogenation of 1,4-diiodo-2,3,5,6-tetraphenylbenzene6, or 10,10’-dibromo-9,9’-bianthryl, polyanthrylene oligomers self-assembled on Au(111), Ag(111) or silica substrates, to name a few examples.

[0020] In some implementations, different pitch and duty cycle combinations in graphene devices are utilized to improve efficiency. In particular, in some implementations, graphene sheets are stacked, with different pitch and critical dimensions, such that devices have multiple pass functionality. Similarly, in some implementations, structures comprising multiple levels of graphene layers allow for more versatile and efficient band gap devices.

[0021] The disclosed implementations are described in the context of methods for fabricating thin films from layered materials and in the context of thin films made therefrom. In this specification and claims, layered materials refer to a material comprising a plurality of sheets, with each sheet having a substantially planar structure.

[0022] As used herein, the term "stacks" refers to one or more sheets of a material (*e.g.*, one or more layers of graphene). For instance, a graphene stack can also refer to one, a few, several, several tens, several hundreds or several thousands sheets of graphene, where each such sheet is a one-atom thick sheet composed of sp^2-hybridized carbon. As used herein, the term "graphene structures" is used interchangeably with "graphene." As used herein, the term "stacks" is interchangeable with the terms "graphene stacks" and "stacks of graphene." In some implementations, a graphene stack in the plurality of graphene stacks includes one or more sheets of graphene. In some implementations, a graphene stack includes between 1 to 500, 5 to 100, or 10 to 50 graphene sheets.

[0023] As used herein, the term "substrate" refers to one layer or multiple layers. In some implementations, a substrate is glass, Si, SiO_2, SiC, or another material. When referring to multiple layers, the term "substrate" is equivalent to and interchangeable with the term "substrate stack." Moreover, it should be understood that the term "substrate" hereinafter refers to any combination of layers upon which additional processing operations are performed. For instance, when one or more layers of a respective material (e.g., SiO_2, Si_3N_4) is grown on a silicon wafer, the term substrate alternatively refers (*e.g.*, depending on context) to the silicon alone or to the silicon wafer inclusive of the one or more layers.

[0024] As used herein, the term "foundation material" refers to any material that is suitable for growing graphene. In some implementations, foundation materials are catalytic metals, *e.g.*, Pt, Au, Fe, Rh, Ti, Ir, Ru, Ni, or Cu. In some other implementations, foundation materials are non-metal materials, such as Si, SiC, non-stoichiometric SiC (*e.g.*, boron doped or

otherwise), and other carbon enhanced materials. As used herein, the phrase "carbon enhanced" materials refers to any materials into which carbon has been added.

[0025] Those of ordinary skill in the art will realize that the following detailed description of the present application is illustrative only and is not intended to be in any way limiting. Other implementations of the present application will readily suggest themselves to such skilled persons having benefit of this disclosure. Reference will now be made in detail to implementations of the present application as illustrated in the accompanying drawings. The same reference indicators will be used throughout the drawings and the following detailed description to refer to the same or like parts.

[0026] In the interest of clarity, not all of the routine features of the implementations described herein are shown and described. It will, of course, be appreciated that in the development of any such actual implementation, numerous implementation-specific decisions must be made in order to achieve the developer's specific goals, such as compliance with application- and business-related constraints, and that these specific goals will vary from one implementation to another and from one developer to another. Moreover, it will be appreciated that such a development effort might be complex and time-consuming, but would nevertheless be a routine undertaking of engineering for those of ordinary skill in the art having the benefit of this disclosure.

[0027] A BSC superconductor is triggered by electron-phonon coupling (EPC). The EPC provides an attractive interaction between electrons at the Fermi surface of a material. When phonon-mediated attraction is strong enough to overcome the Coulombic repulsion between electrons, the electrons form "Cooper pairs", leading to the emergence of superconductivity below a critical temperature T_c. The critical temperature T_c for a material increases when the Fermi surface of a material increases and the EPC of the material increases. Increases in the Fermi surface enable more Cooper pairs to form, and increases in the EPC enable easier Cooper pair formation. Equation (1) provided below provides the general scaling relationship of the critical temperature of a material as a function of the Fermi surface and EPC.

$$T_c \sim \exp\left[-\frac{1}{\lambda}\right] \sim \exp\left[-\frac{1}{N(0)V_{ep}}\right], \qquad (1)$$

where, the dimensionless parameter λ characterizes the overall EPC strength, $N(0)$ is the electron DOS and V_{ep} is the unit electron-phonon pairing potential at the Fermi level. Generally, the EPC of a material can be classified into three regimes: weak $\lambda \ll 1$, intermediate $\lambda \sim 1$, and strong $\lambda > 1$. Generally, a good BCS superconductor requires $\lambda \geq 1$.

[0028] The EPC of a material plays an important role in determining electron transport properties through electron-phonon scattering as well as giving rise to exotic many-body phenomenon, such as superconductivity. However, the EPC of intrinsic graphene is very weak because of a diminishing Fermi surface (a point for intrinsic graphene) and a very weak electron-phonon pairing potential (because of the high Fermi temperature of the massless carriers and high energy of the optical phonons). On the one hand, the weak EPC is responsible for some of the many distinguishing properties graphene has, such as extremely high electrical and thermal conductivity. On the other hand, the weak EPC prevents graphene from being a superconductor.

[0029] With reference to equation (1), the EPC of graphene (λ) can be increased by increasing at least one of the electron DOS [$N(0)$] and the electron-phonon pairing potential (V_{ep}) at the Fermi level. Given the linear Dirac states around Fermi level and electron-hole symmetry, $N(0)$ can be increased by doping of either electrons and holes. Figure 1a shows calculated results of $N(0)$ and λ as a function of hole concentration for p-type graphene (e.g., graphene doped with a material providing holes). Under doping the peculiar point-like Fermi surface of intrinsic graphene evolves into a Fermi circle, the Fermi surface grows, and, in turn, $N(0)$ increases linearly with the doping level, until a maximum doping level is reached. The increase of $N(0)$ directly enhances the EPC and the value of λ is calculated to be ~0.22 at the doping level of 7.63×10^{14} cm^{-2}. This is consistent with previous theoretical prediction: an approximated relation between λ and the number of free (doped) carriers per unit cell n is given by $\lambda = 0.34\sqrt{n}$, which gives $\lambda = 0.215$ for the same doping level. However, even at this relatively high doping level, λ remains within the weak coupling regime.

[0030] Also, from Fig. 1a, λ is seen to increase linearly with the increasing doping level, the same as $N(0)$. Since $\lambda = N(0)V_{ep}$, this indicates that V_{ep} remains a constant, ~ 0.5 eV as shown in the inset of Fig. 1a, independent of doping. This value of V_{ep} for graphene is much smaller than the typical values found in conventional BCS superconductors, such as 1.4 eV for MgB_2 and 3 eV for Boron-doped (B-doped) diamond.

[0031] The results of Fig. 1a show that doping alone cannot make graphene a BCS superconductor. One reason is that, although doping enlarges the Fermi surface, λ remains in the weak coupling regime because V_{ep} for graphene is independent of doping and is very small. Another is that even though EPC strength, λ, increases linearly with the doping level it is not possible to dope at a high enough level to increase EPC into the good superconducting regime with λ close to 1.

[0032] As provided for in some implementations, graphene is adapted to increase the electron-phonon pairing potential V_{ep} in addition to and/or as an alternative to charge doping. In some implementations, applying tensile strain to graphene is used to weaken carbon-carbon (C-C) bonds and hence lower the optical phonon energy. As described in greater detail below, first-principles calculations show uniform phonon mode softening under tensile strain. Furthermore, tensile strain tends to enhance the Kohn anomaly in graphene, which in turn produces increases in EPC strength. In order to demonstrate the relationship between the electron-phonon pairing potential V_{ep} and tensile strain, V_{ep} was determined for a range of strain values. Fig. 1b illustrates the results of calculations for the V_{ep} of graphene as a function of biaxial tensile strain for a hole-doped (e.g, p-type) graphene with a doping level of 4.58×10^{14} cm^{-2}. As illustrated in Fig. 1b, V_{ep} increases substantially with the increasing strain. In particular, at the 16.5% of strain, V_{ep} reaches as high as 3.3 eV, which is even larger than that in the B-doped diamond.

[0033] Consequently, in some implementations, the combined effects of charge doping and strain are used in the methods and apparatus of the instant disclosure to drive graphene into the strong coupling regime of λ and thus enable graphene-based superconductors that operate at a critical temperature T_c substantially above zero Kelvin. To that end, Fig. 2(a) illustrates values for λ calculated as a function of hole doping and tensile strain. At threshold high doping levels and strains, λ becomes larger than 1.0, indicating that the EPC of graphene is in the strong coupling regime, which will trigger superconductivity at a critical temperature T_c substantially above zero Kelvin.

[0034] In accordance with some implementations, an estimate of the critical temperature T_c is obtained using the McMillan-Allen-Dynes formula, provided as equation (2) as follows:

$$T_c = \frac{\hbar\omega_{log}}{1.2k_B} \exp\left[\frac{-1.04(1+\lambda)}{\lambda-\mu^*(1+0.62\lambda)}\right] \quad (2)$$

where ω_{log} is the logarithmically averaged phonon frequency, μ^* is the screened electron Coulomb pseudo-potential, which is known to be in the order of 0.1 in most *sp*-electron metals. Here, μ^*=0.115, as extracted from fitting the experimental critical temperature of CaC_6. Fig. 2(b) shows T_c as a function of hole doping and tensile strain. The critical temperature T_c increases monotonically with both the increasing doping level at the given strain level and the increasing strain level at the given doping level. At the 16.5% strain, T_c can reach as high as 18.6 K, 23.0 K and 30.2 K for the doping level of 1.52×10^{14}, 4.58×10^{14} and 7.63×10^{14} cm^{-2}, respectively.

[0035] To better understand the underlying physical mechanisms of strain enhanced λ, Figs. 3(a), (c) and (e) show the Eliashberg function of equation (3):

$$\alpha^2F(\omega) = \frac{1}{N(0)}\sum_{m}^{n}\sum_{q}^{\nu}\delta(\omega-\omega_{q\nu})\sum_{k}|g_{k+q,k}^{q\upsilon,mn}|^2\delta(\varepsilon_{k+q,m}-\varepsilon_F)\delta(\varepsilon_{k,n}-\varepsilon_F) \quad (3)$$

and the frequency-dependent EPC function of equation (4)

$$\lambda(\omega) = 2\int\frac{\alpha^2F(\omega)}{\omega}d\omega^{23} \quad (4)$$

where phonon frequencies ω are indexed with wavevector (q) and mode number (ν), and the electron eigenvalues ε are indexed with wavevector (k) and the band indices (m and n), and $g_{k+q,k}^{q\upsilon,mn}$ represents the electron-phonon matrix element. The Eliashberg function is found sharply peaked at certain energy having a δ-like shape. For clarity, the peak that dominates the EPC has been shaded. It corresponds to the SH*(shear horizontal optical) in-plane C-C stretching phonon mode. As the tensile strain increases, the shaded peak moves towards to the lower energy, due to the softening of this particular phonon mode. Because of the $1/\omega$ scaling of λ(ω) [Eq. (3)], the red shift of the this peak under strain results in the shape increase of λ, especially for large strain as shown in Fig. 1(b).

[0036] In accordance with some implementations, λ is expressed rigorously by $\lambda = N(0)\langle g^2\rangle/M\langle\omega^2\rangle$, where $\langle g^2\rangle$ is the average of the squared electronic matrix element over the Fermi surface, M is the atomic mass, and $\langle\omega^2\rangle$ is the average of the squared phonon frequency:

$$\langle\omega^2\rangle = \int d\omega\,\omega\,\alpha^2\,F(\omega)/\int\frac{d\omega\,\alpha^2F(\omega)}{\omega}.$$

In view of the δ-like shape of Eliashberg function, effectively only one characteristic phonon mode with energy (ω_0) dominates the EPC contributing to λ, like the Einstein mode. Thus $\langle\omega^2\rangle$ can be simplified as ω_0^2, and the value of $\langle\omega^2\rangle^{1/2}$ can be therefore used to characterize the dominating phonon energy ω_0. Figs. 3(b), (d) and (f) show the calculated $\langle\omega^2\rangle^{1/2}$ as a function of tensile strain (ε) for three hole doped graphene, in which $\langle\omega^2\rangle^{1/2}$ is linear with the increasing ε.

[0037] This can be simply understood as follows. Under the biaxial tensile strain, the characteristic phonon energy can be approximated as changing as $\omega_{0,\varepsilon} = \omega_0 - \frac{\partial\omega_{0,\varepsilon}}{\partial\varepsilon}\varepsilon$, where $\frac{\partial\omega_{0,\varepsilon}}{\partial\varepsilon}$ is the phonon deformation potential. Thus, it is the linearly decreasing ω_0 under tensile strain that increases V_{ep} and λ. This is further shown by plotting λ versus $\langle\omega^2\rangle^{-2}$. *See* insets of the Figs. 3(b), (d) and (f)], which display a good linear relation. This also implies that $N(0)\langle g^2\rangle$ remains almost constant at given range of doping, independent of tensile strain.

[0038] Accordingly, in view of at least the foregoing, it has been demonstrated that charge doping and tensile strain greatly enhances λ: the former provides enough carriers, and the latter increases EPC. At a given doping level, although λ increases monotonically with the increasing strain, it is worth pointing out that T_c will not increase indefinitely with strain. Looking at the McMillan-Allen-Dynesformula [Eq. (2)] again, it is noted that the T_c is bounded by two parameters at given μ^*, λ and ω_{log}. Taking the 4.58×10^{14} cm^{-2} hole-doped graphene as an example, Fig. 4 shows ω_{log} as a function of ε. It is seen that ω_{log} decreases as ε increase, which is related to the decrease of the characteristic phonon energy ω_0. The opposite variation of λ versus ω_{log} under strain indicates that T_c would reach a maximum value at a certain strain. This is seen in Fig. 2(c), where T_c increases continuously from 0.3 K to 30.2 K when ε increases from 10% to 16.5%, but decreases slightly from 30.2 K to 29.2 K when ε further increases from 16.5% to 17%, even though λ increases continuously in all range of strains. It indicates that first the increase of λ dominates the increase of T_c, and then the decrease of ω_{log} hinders the further increase of T_c.

[0039] In some implementations, due to high hole-electron symmetry at the Dirac point, charge doped (n-type or p-ytpe) graphene under tensile strain will demonstrate a similar superconductivity transition. Table 1 shows λ, ω_{log} and T_c at different biaxial tensile strains for

the 4.58×10^{14} cm^{-2} electron-doped graphene. Over the range of strain values presented both λ and T_c increase with the increasing strain. Notably, as the strain increases from 12% to 15.6%, the T_c jumps from 0.2 K to as high as 22.4 K.

Table 1: λ, ω_{log} and T_c of 3% electron-doped graphene under biaxial tensile strain

strain(ε)	λ	ω_{log} (cm^{-1})	T_c (K)
0.0%	**0.10**	**1072.3**	**0**
12%	**0.30**	**526.1**	**0.2**
14%	**0.48**	**367.5**	**4.2**
15%	**0.75**	**266.9**	**13.8**
15.6%	**1.20**	**185.5**	**22.4**

[0040] In some implementations, doping levels above 10^{14} cm^{-2} in graphene can be achieved by either chemical doping or electrical doping. Additionally and/or alternatively, in some implementations, graphene is able to sustain up to 20% tensile strain without breaking. Additionally and/or alternatively, in some implementations, doping is used to further strengthen graphene so that the doped graphene able to sustain levels of strain greater than 20%.

[0041] In some implementations, the superconductivity transition of doped graphene is triggered at least by enhancing EPC using a force to create tensile strain, which is different from the transition observed in metal-decorated graphene. The enhancement of EPC λ in metal-decorated graphene arises from additional metal-related electronic states around the Fermi level, which will couple strongly with low-frequency out-of-plan modes of graphene and the phonon modes of adsorbed metal. From this perspective, metal-decorated graphene is similar to intercalated graphite and to MgB_2.

[0042] By contrast, based on the implementations disclosed herein, enhancement of EPC λ arises from the combined effect of doping and tensile strain. Tensile strain modifies the electronic structure of graphene by changing the slope of the π band, leading to a change of Fermi velocity. Nevertheless the electrons scattered by the phonons consist of the π electrons, e.g, 2D massless Dirac fermions. As such, implementations of the graphene superconductor disclosed herein are different from doped graphene up to the van Hove singularity point with a very high doping level. In the latter, the electron DOS diverges logarithmically, which greatly increases electronic many-body interaction that may trigger a chiral superconductor by any arbitrary electron-electron attraction with an unknown but likely low T_c.

[0043] It will also be understood that, although the terms "first," "second," etc. may be used herein to describe various elements, these elements should not be limited by these terms. These terms are only used to distinguish one element from another. For example, a first contact could be termed a second contact, and, similarly, a second contact could be termed a first contact, which changing the meaning of the description, so long as all occurrences of the "first contact" are renamed consistently and all occurrences of the second contact are renamed consistently. The first contact and the second contact are both contacts, but they are not the same contact.

[0044] The terminology used herein is for the purpose of describing particular embodiments only and is not intended to be limiting of the claims. As used in the description of the embodiments and the appended claims, the singular forms "a", "an" and "the" are intended to include the plural forms as well, unless the context clearly indicates otherwise. It will also be understood that the term "and/or" as used herein refers to and encompasses any and all possible combinations of one or more of the associated listed items. It will be further understood that the terms "comprises" and/or "comprising," when used in this specification, specify the presence of stated features, integers, steps, operations, elements, and/or components, but do not preclude the presence or addition of one or more other features, integers, steps, operations, elements, components, and/or groups thereof.

[0045] As used herein, the term "if" may be construed to mean "when" or "upon" or "in response to determining" or "in accordance with a determination" or "in response to detecting," that a stated condition precedent is true, depending on the context. Similarly, the phrase "if it is determined [that a stated condition precedent is true]" or "if [a stated condition precedent is true]" or "when [a stated condition precedent is true]" may be construed to mean "upon determining" or "in response to determining" or "in accordance with a determination" or "upon detecting" or "in response to detecting" that the stated condition precedent is true, depending on the context.

[0046] The foregoing description, for purpose of explanation, has been described with reference to specific embodiments. However, the illustrative discussions above are not intended to be exhaustive or to limit the invention to the precise forms disclosed. Many modifications and variations are possible in view of the above teachings. The embodiments were chosen and

described in order to best explain the principles of the invention and its practical applications, to thereby enable others skilled in the art to best utilize the invention and various embodiments with various modifications as are suited to the particular use contemplated.

What is claimed is:

1. A method of producing a graphene-based superconductive device comprising:

providing a stack of charge doped graphene characterized by a doping level, in at least a portion of the stack, that exceeds a threshold doping level; and

imposing a strain on the charge doped graphene to produce a tensile strain ε in the stack of charge doped graphene, wherein the tensile strain ε exceeds a threshold strain level, and

wherein the combination of the threshold doping level and the threshold strain level cause the critical temperature of the stack of charge doped graphene to exceed 3.0 Kelvin.

2. The method of claim 1, wherein the threshold strain level is between five percent and twenty percent.

3. The method of claim 1, wherein the threshold strain level is between ten percent and twenty percent.

4. The method of claim 1, wherein the threshold strain level is between fifteen percent and twenty percent.

5. The method of claim 1, wherein the threshold strain level is five percent.

6. The method of claim 1, wherein the combination of the threshold doping level and the threshold strain level cause the critical temperature of the stack of charge doped graphene to exceed 8.0 Kelvin.

7. The method of claim 1, wherein the combination of the threshold doping level and the threshold strain level cause the critical temperature of the stack of charge doped graphene to exceed 12.0 Kelvin.

8. The method of claim 1, wherein the combination of the threshold doping level and the threshold strain level cause the critical temperature of the stack of charge doped graphene to exceed 16.0 Kelvin.

9. The method of claim 1, wherein the combination of the threshold doping level and the threshold strain level cause the critical temperature of the stack of charge doped graphene to exceed 20.0 Kelvin.

10. The method of claim 1, wherein the combination of the threshold doping level and the threshold strain level cause the critical temperature of the stack of charge doped graphene to exceed 25.0 Kelvin.

11. The method of claim 1, wherein the threshold doping level is $\sim 3.5\times 10^{14}$ cm^{-2} holes.

12. The method of claim 1, wherein the threshold doping level is $\sim 4.0\times 10^{14}$ cm^{-2} holes.

13. The method of claim 1, wherein the threshold doping level is $\sim 5.0\times 10^{14}$ cm^{-2} holes.

14. The method of claim 1, wherein the threshold doping level is $\sim 6.0\times 10^{14}$ cm^{-2} holes.

15. The method of claim 1, wherein the threshold doping level is $\sim 7.0\times 10^{14}$ cm^{-2} holes.

16. The method of claim 1, wherein the threshold doping level is $\sim 8.0\times 10^{14}$ cm^{-2} holes.

17. The method of claim 1, wherein the stack of charge doped graphene is n-type doped.

18. The method of claim 1, wherein the stack of charge doped graphene is p-type doped.

19. The method of claim 1, wherein the stack of charge doped graphene is electron-doped graphene.

20. The method of claim 1, wherein the stack of charge doped graphene is chemical-doped graphene.

21. The method of claim 1, wherein the tensile strain is biaxial.

22. The method of claim 1, wherein the tensile strain is substantially along one axis characterizing the stack of charge doped graphene.

23. The method of claim 1, wherein the threshold strain level is between 10% and 20%.

24. The method of claim 1, wherein the threshold doping level is between 10^{13} cm^{-2} and 10^{15} cm^{-2}.

25. The method of claim 1, wherein the doping level increases the amount of strain that intrinsic graphene can tolerate before breaking.

26. A graphene-based superconductive device comprising:

a stack of charge doped graphene characterized by a doping level, in at least a portion of the stack, that exceeds a threshold doping level; and

a force transference structure that engages respectively at least two portions of the stack of charge doped graphene, thereby imposing a force into the stack of charge doped graphene that imposes a tensile strain ε in the stack of charge doped graphene, wherein the tensile strain ε exceeds a threshold strain level,

wherein the combination of the threshold doping level and the threshold tensile strain level cause the critical temperature of the stack of charge doped graphene to exceed 3.0 Kelvin.

27. The graphene-based superconductive device of claim 26, wherein the threshold strain level is between five percent and twenty percent.

28. The graphene-based superconductive device of claim 26, wherein the threshold strain level is between ten percent and twenty percent.

29. The graphene-based superconductive device of claim 26, wherein the threshold strain level is between fifteen percent and twenty percent.

30. The graphene-based superconductive device of claim 26, wherein the threshold strain level is five percent.

31. The graphene-based superconductive device of claim 26, wherein the combination of the threshold doping level and the threshold strain level cause the critical temperature of the stack of charge doped graphene to exceed 8.0 Kelvin.

32. The graphene-based superconductive device of claim 26, wherein the combination of the threshold doping level and the threshold strain level cause the critical temperature of the stack of charge doped graphene to exceed 12.0 Kelvin.

33. The graphene-based superconductive device of claim 26, wherein the combination of the threshold doping level and the threshold strain level cause the critical temperature of the stack of charge doped graphene to exceed 16.0 Kelvin.

34. The graphene-based superconductive device of claim 26, wherein the combination of the threshold doping level and the threshold strain level cause the critical temperature of the stack of charge doped graphene to exceed 20.0 Kelvin.

35. The graphene-based superconductive device of claim 26, wherein the combination of the threshold doping level and the threshold strain level cause the critical temperature of the stack of charge doped graphene to exceed 25.0 Kelvin.

36. The graphene-based superconductive device of claim 26, wherein the threshold doping level is $\sim 3.5 \times 10^{14}$ cm^{-2} holes.

37. The graphene-based superconductive device of claim 26, wherein the threshold doping level is $\sim 4.0 \times 10^{14}$ cm^{-2} holes.

38. The graphene-based superconductive device of claim 26, wherein the threshold doping level is $\sim 5.0 \times 10^{14}$ cm^{-2} holes.

39. The graphene-based superconductive device of claim 26, wherein the threshold doping level is $\sim 6.0 \times 10^{14}$ cm^{-2} holes.

40. The graphene-based superconductive device of claim 26, wherein the threshold doping level is $\sim 7.0 \times 10^{14}$ cm^{-2} holes.

41. The graphene-based superconductive device of claim 26, wherein the threshold doping level is $\sim 8.0 \times 10^{14}$ cm^{-2} holes.

42. The graphene-based superconductive device of claim 26, wherein the stack of charge doped graphene is n-type doped.

43. The graphene-based superconductive device of claim 26, wherein the stack of charge doped graphene is p-type doped.

44. The graphene-based superconductive device of claim 26, wherein the stack of charge doped graphene is electron-doped graphene.

45. The graphene-based superconductive device of claim 26, wherein the stack of charge doped graphene is chemical-doped graphene.

46. The graphene-based superconductive device of claim 26, wherein the tensile strain is biaxial.

47. The graphene-based superconductive device of claim 26, wherein the tensile strain is substantially along one axis characterizing the stack of charge doped graphene.

48. The graphene-based superconductive device of claim 26, wherein the threshold strain level is between 10% and 20%.

49. The graphene-based superconductive device of claim 26, wherein the threshold doping level is between 10^{13} cm^{-2} and 10^{15} cm^{-2}.

50. The graphene-based superconductive device of claim 26, wherein the doping level increases the amount of strain that intrinsic graphene can tolerate before breaking.

51. The graphene-based superconductive device of claim 26, wherein the force transference structure includes a first rigid element and a second rigid element that respectively engage the at least two portions of the stack of charge doped graphene.

52. The graphene-based superconductive device of claim 26, wherein:

the first rigid element includes two planar sub-elements, each of the two planar subelements having a respective aperture, and the stack of charge doped graphene is arranged between the two planar sub-elements and substantially exposed by the respective apertures of the two planar sub-elements; and

the second rigid element is operable to engage the exposed portion of the stack of charge doped graphene to impart the force causing the tensile strain.

53. A method of producing a graphene-based superconductive device comprising:

providing a stack of charge doped graphene characterized by a doping level within a threshold doping range; and

imparting a force to the stack of charge doped graphene to produce tensile strain in the stack of charge doped graphene, wherein the tensile strain is characterized by a strain level within a threshold strain range,

wherein the combination of the doping level and strain level determine the critical temperature of the stack of charge doped graphene.

54. The method of claim 1, wherein the stack of charge doped graphene consists of between 2 and 1000 graphene sheets.

55. The method of claim 1, wherein the stack of charge doped graphene consists of between 10 and 500 graphene sheets.

56. The method of claim 1, wherein the stack of charge doped graphene consists of between 30 and 250 graphene sheets.

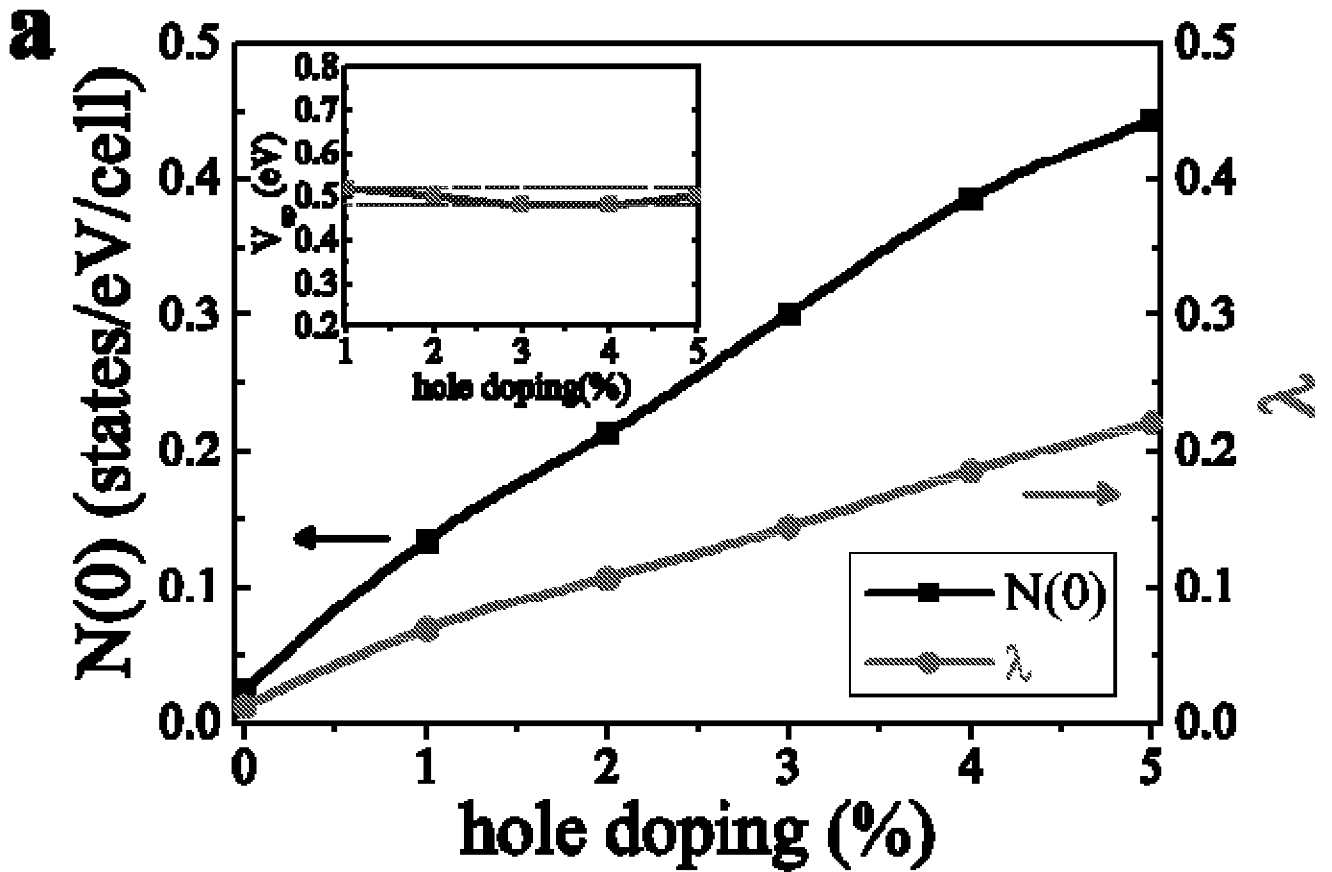

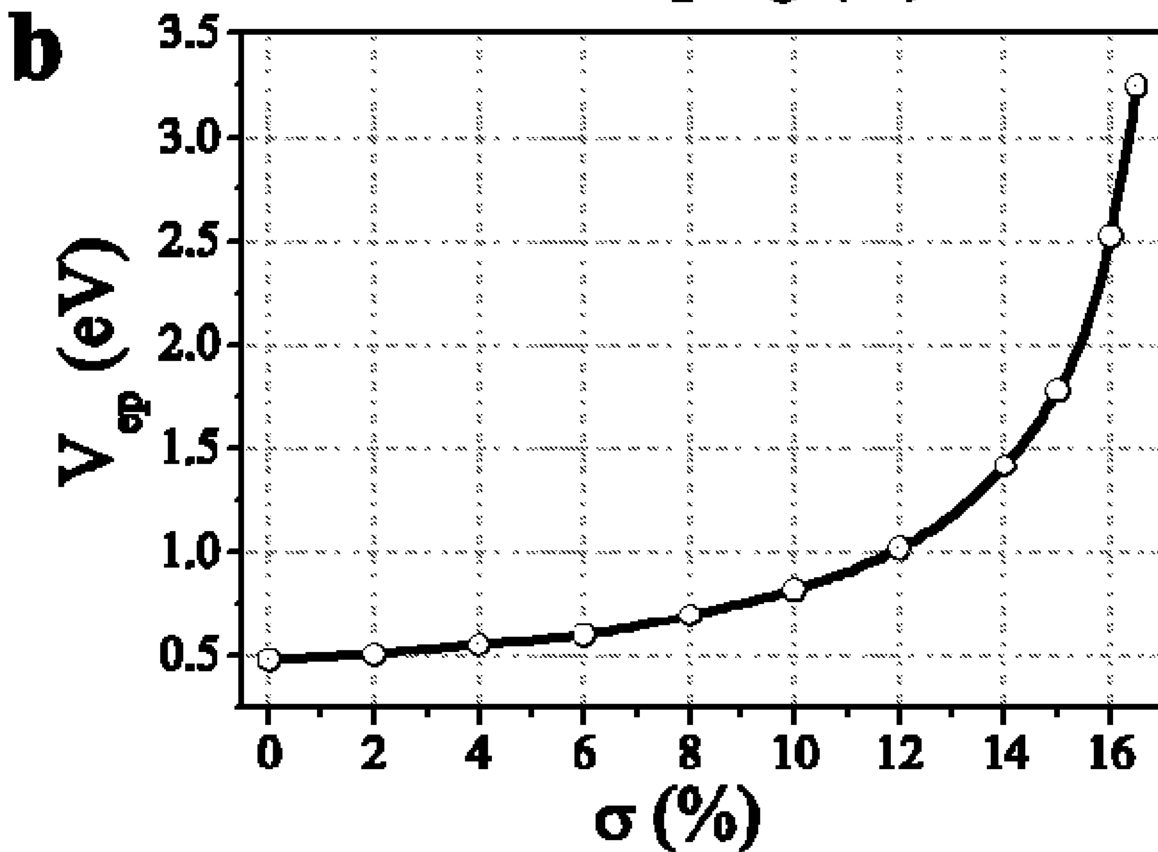

FIGURE 1

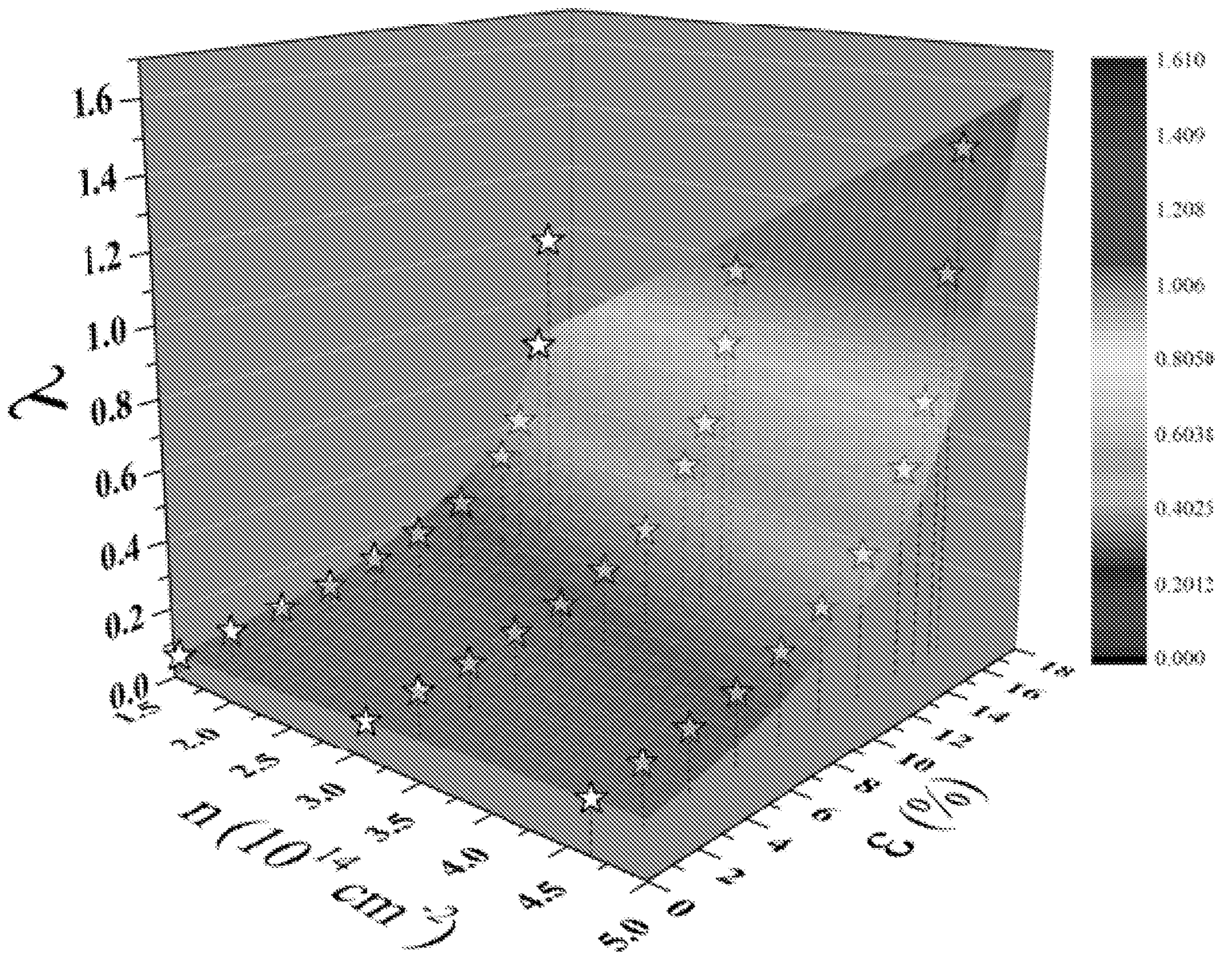

Figure 2(a)

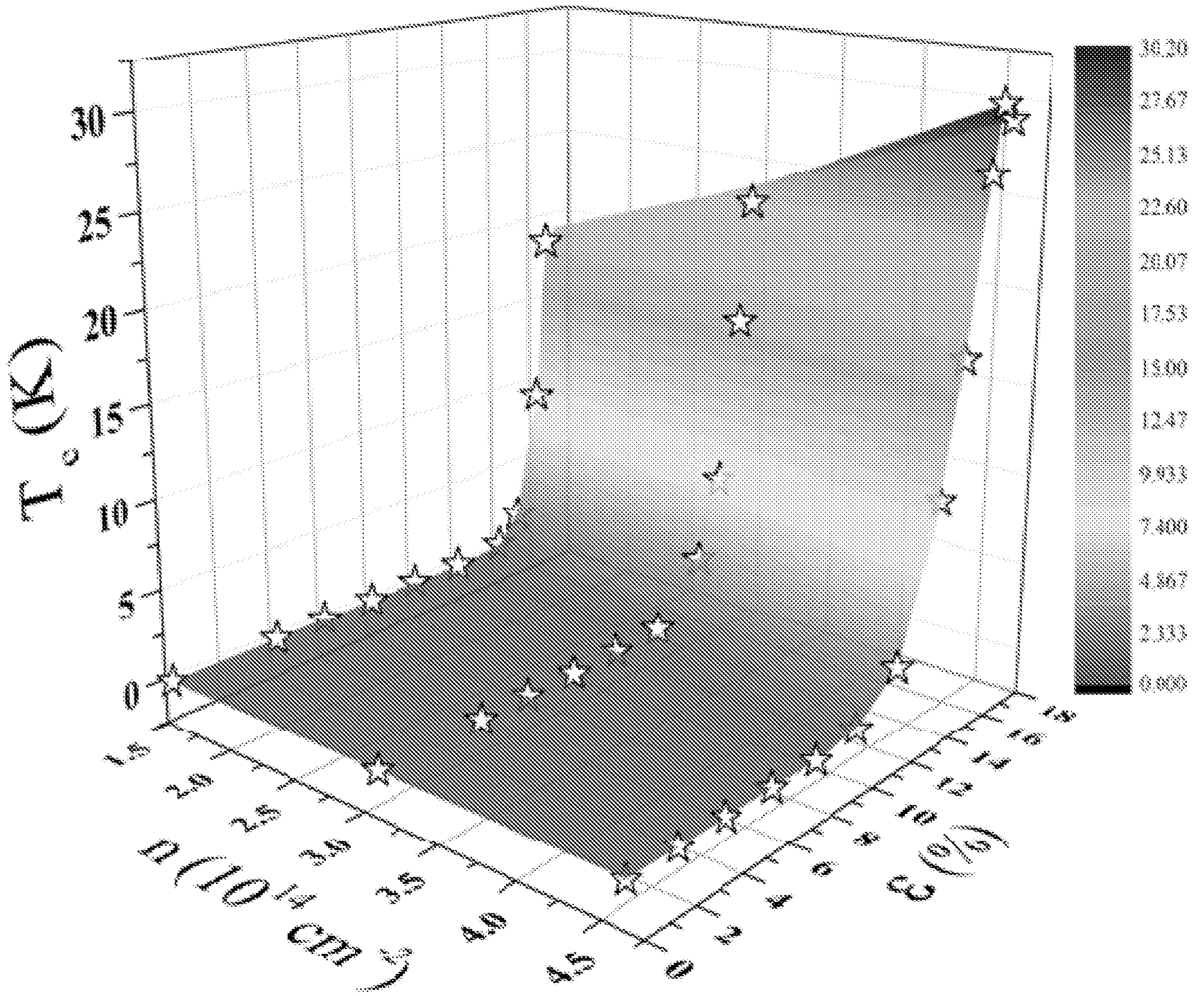

Figure 2(b)

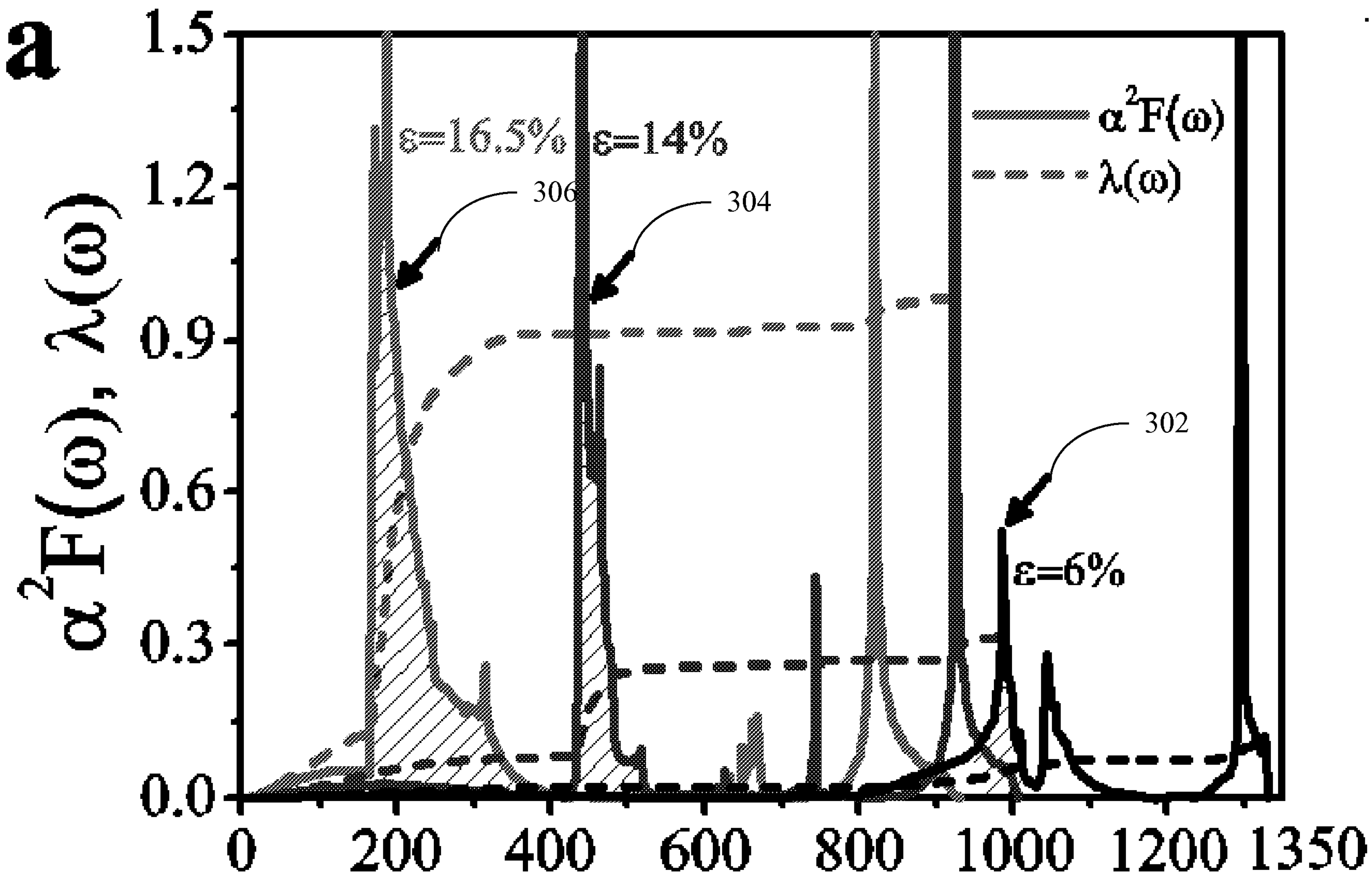

Figure 3(a)

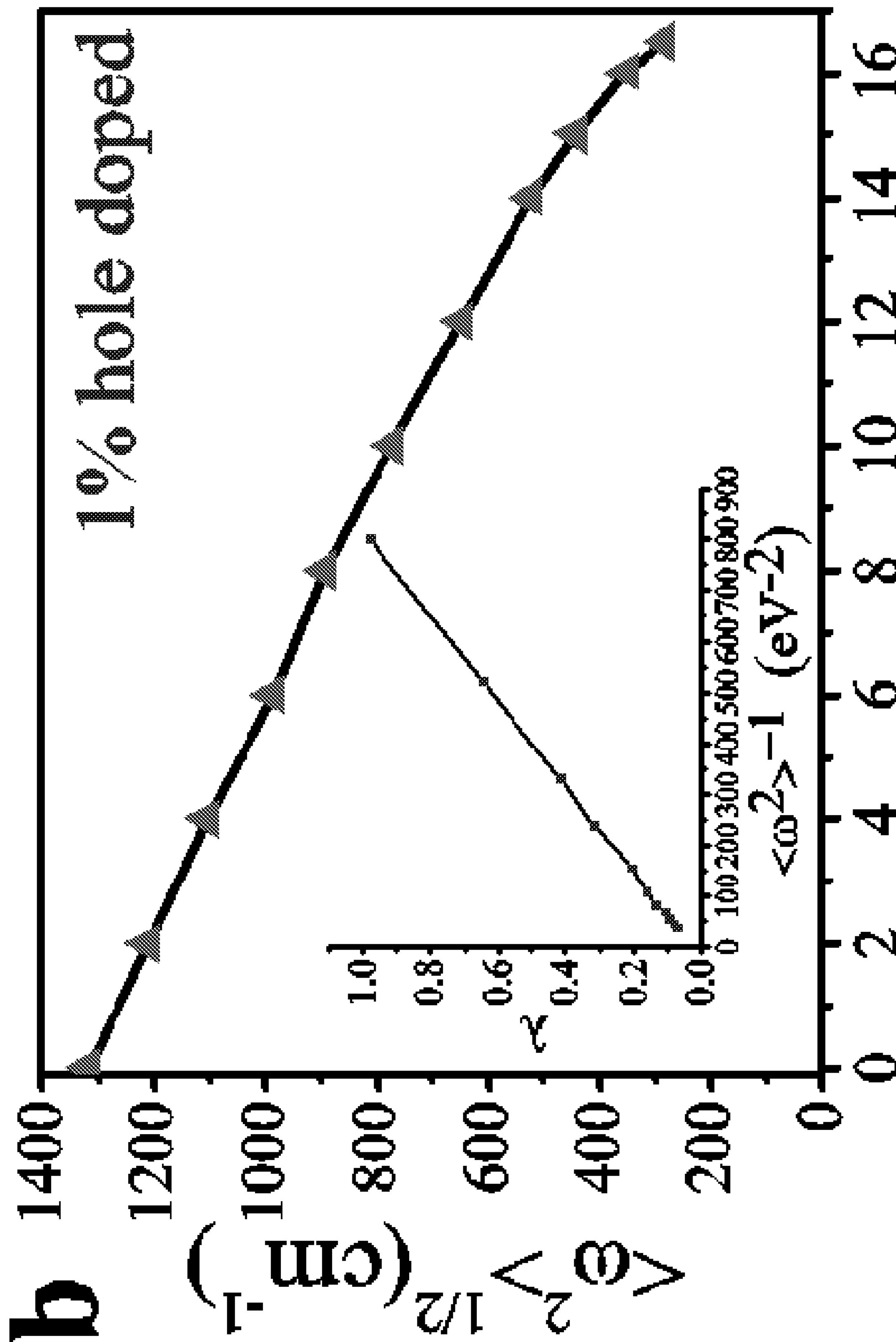

Figure 3(b)

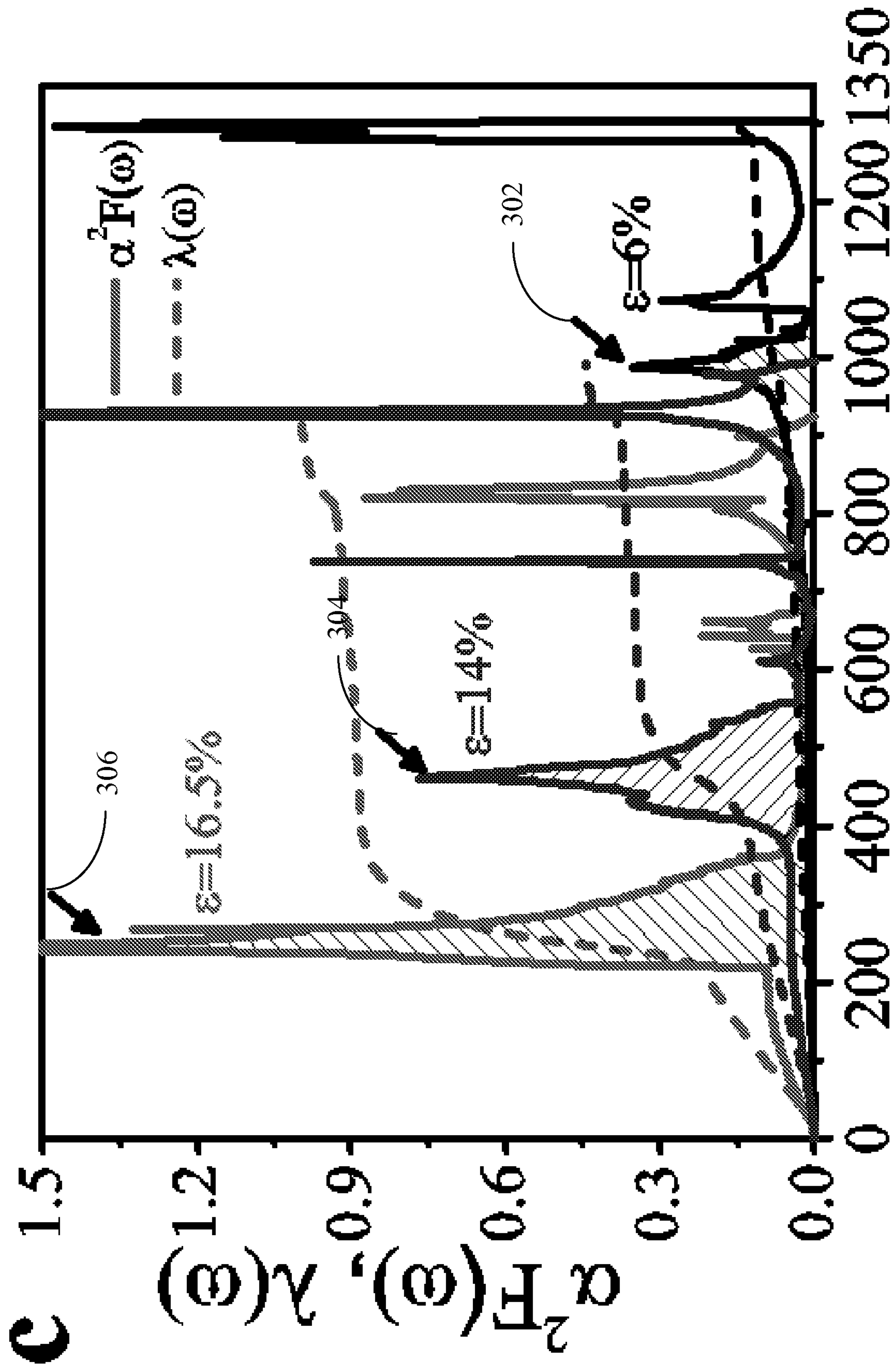

Figure 3(c)

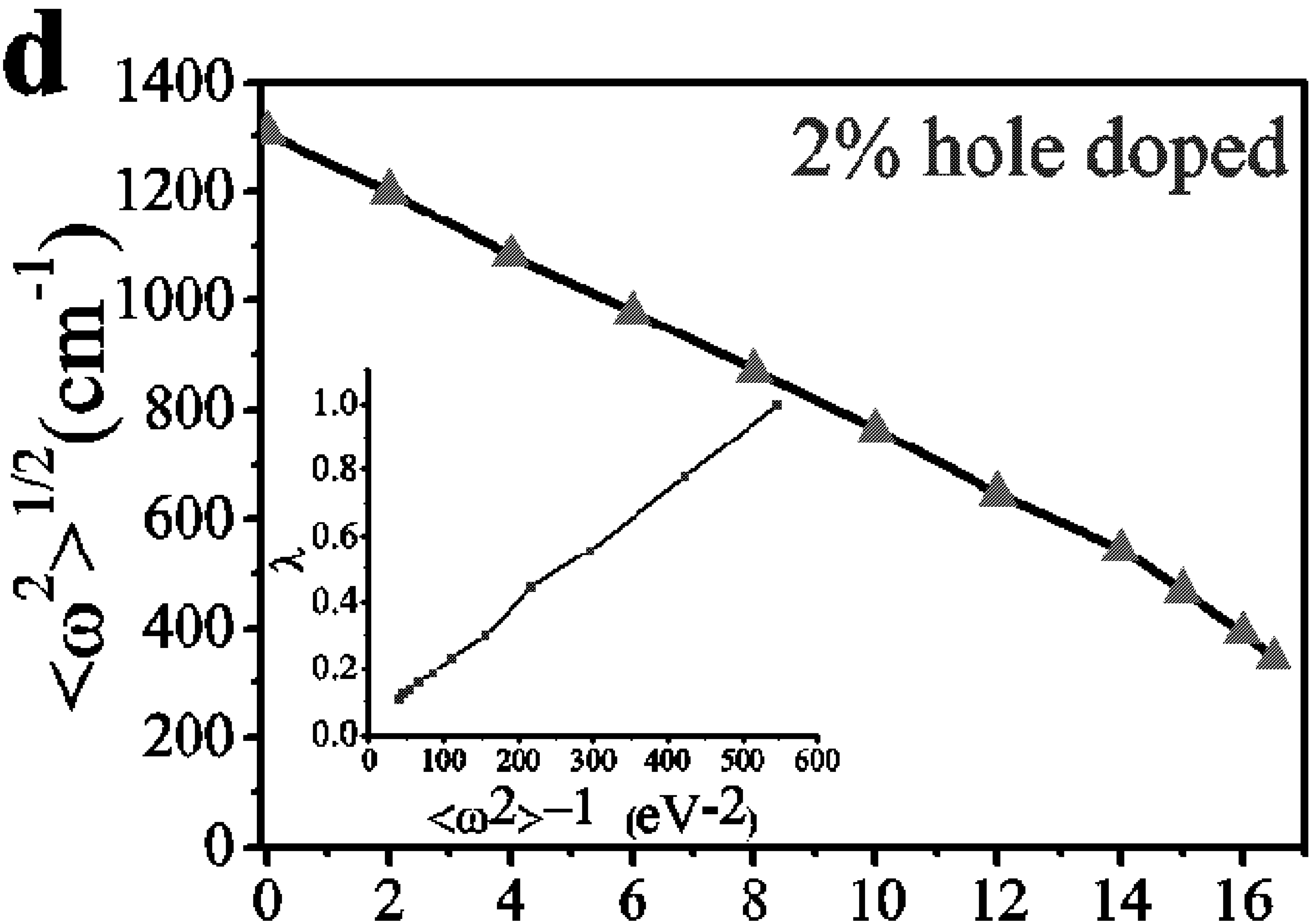

Figure 3(d)

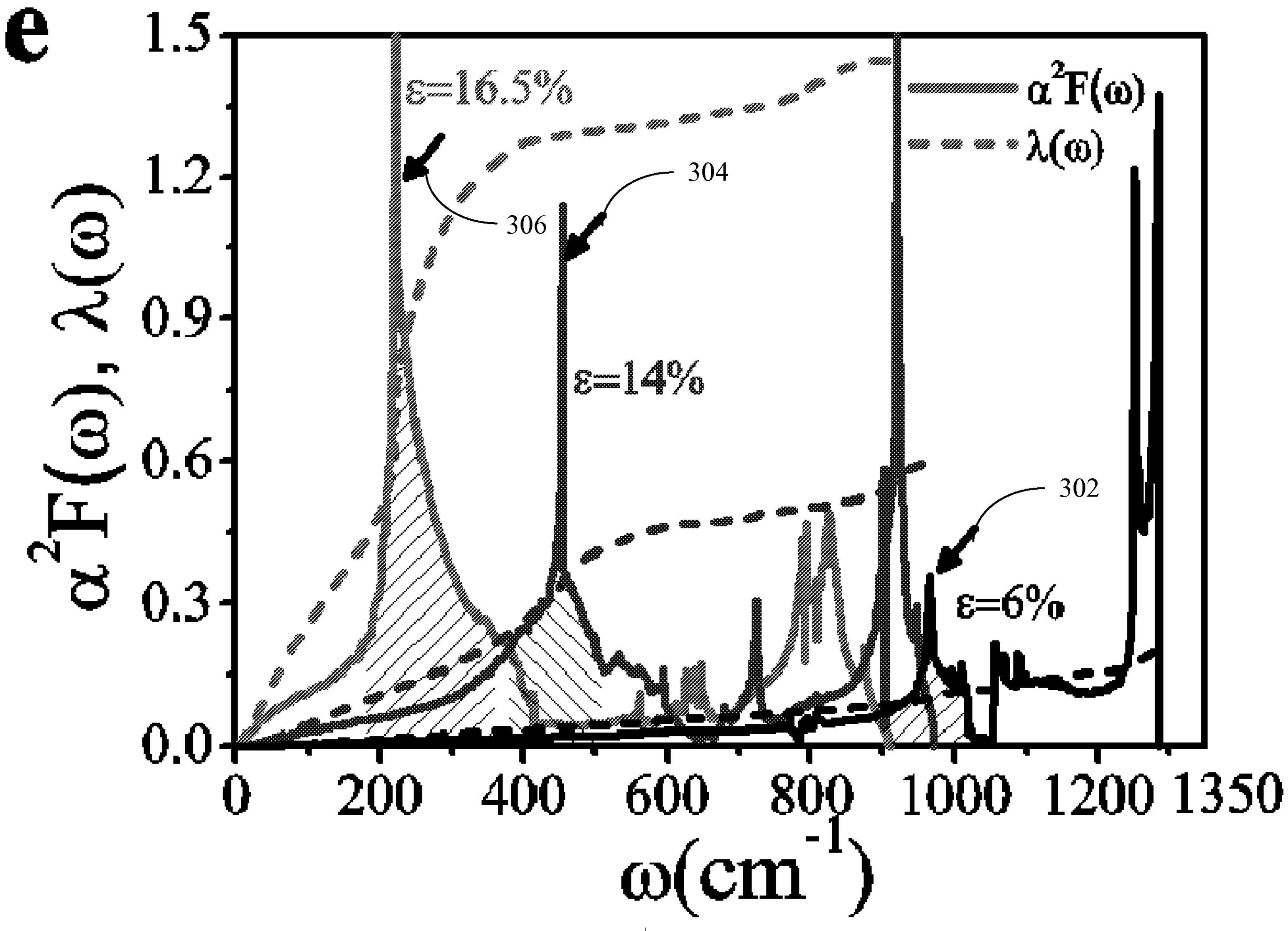

Figure 3(e)

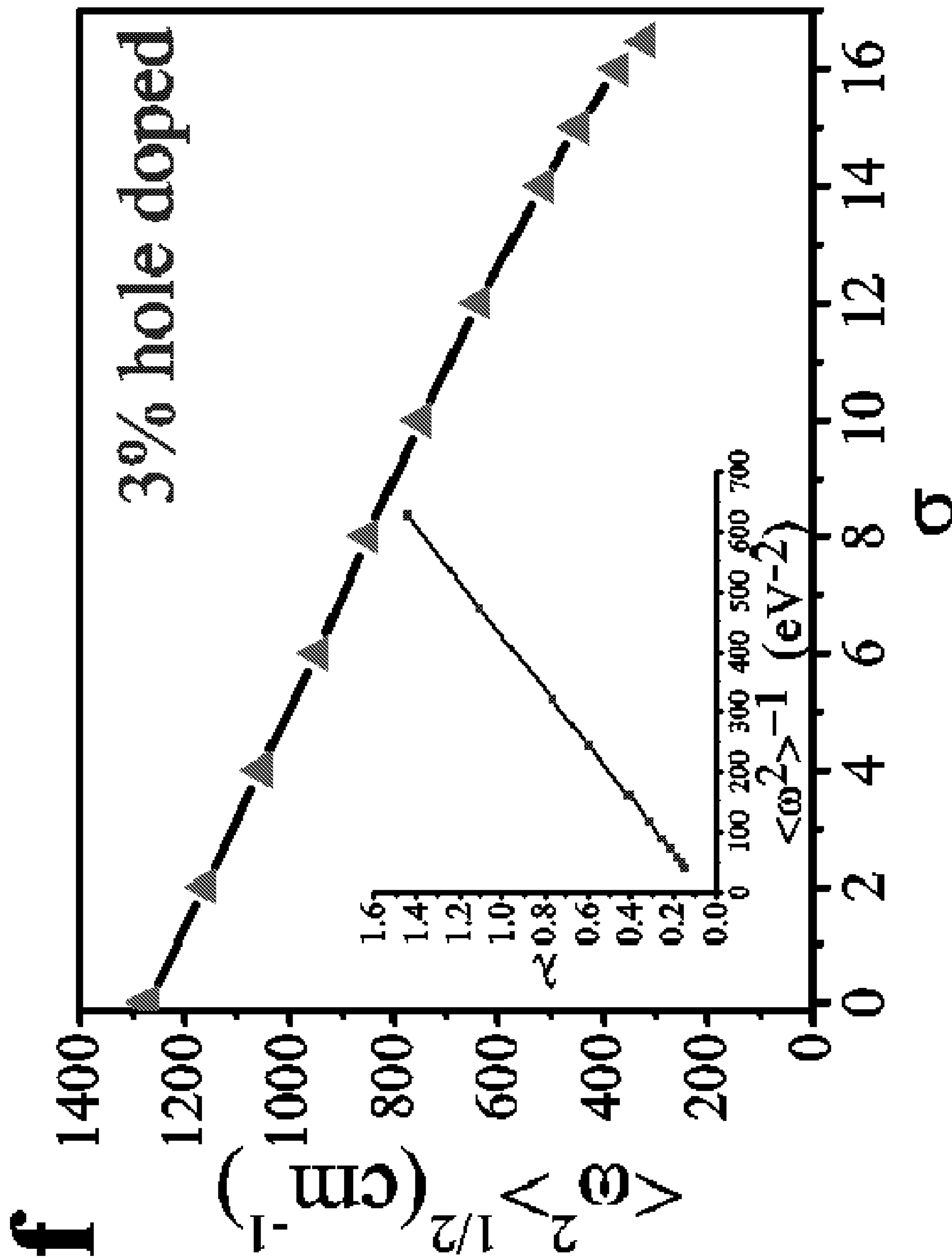

Figure 3(f)

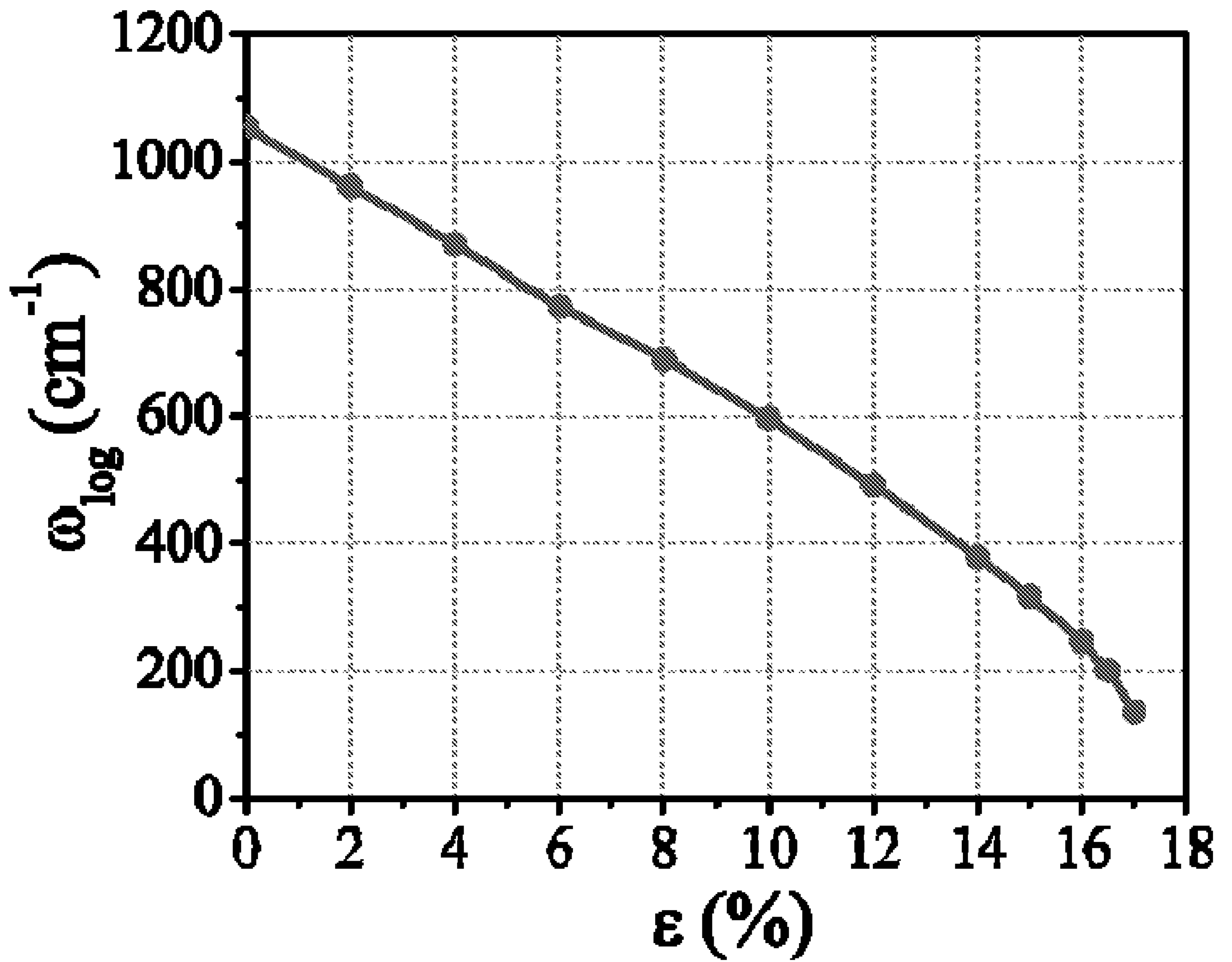

Figure 4

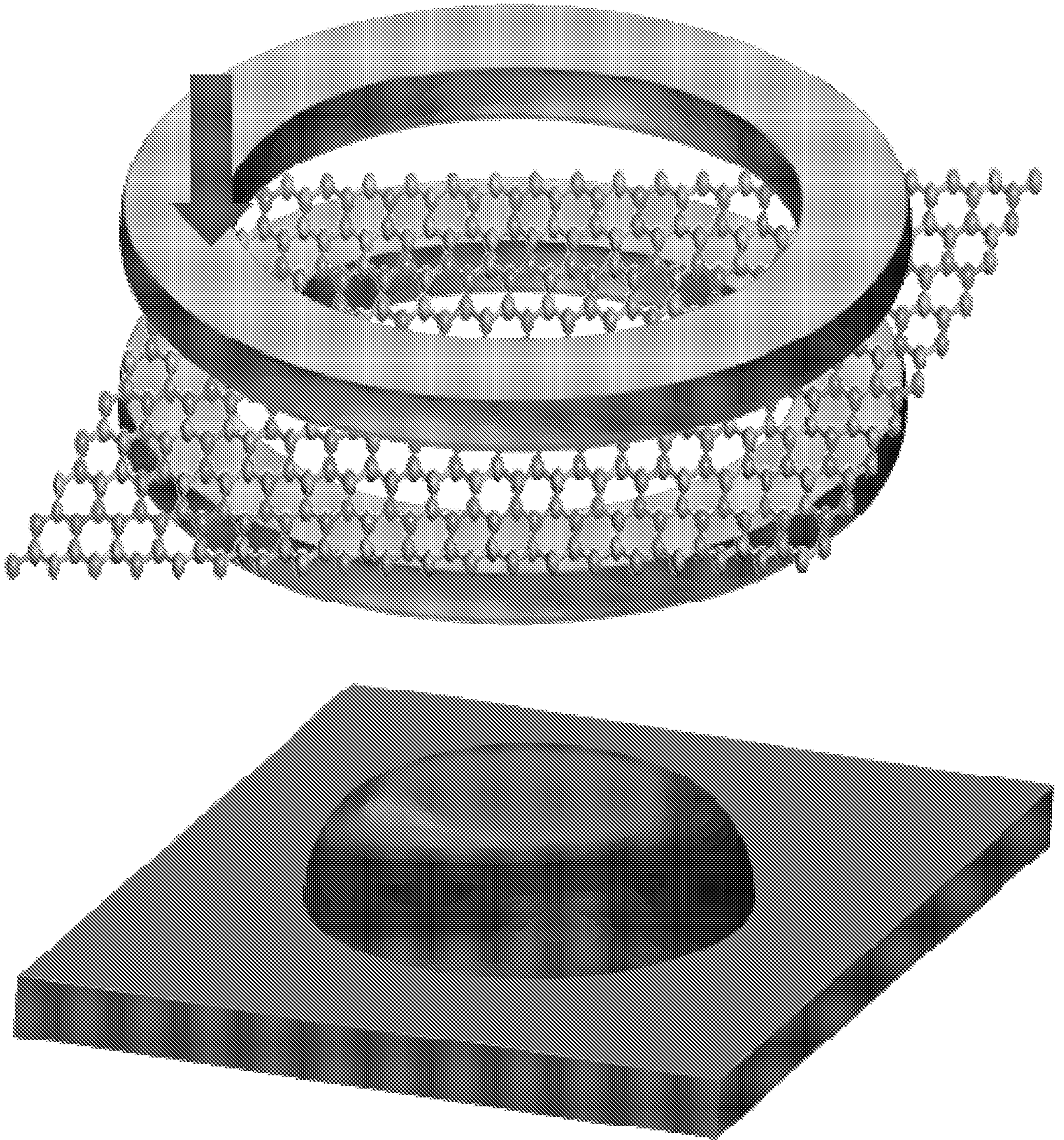

Figure 5

INTERNATIONAL SEARCH REPORT

International application No.
PCT/US2014/030887

A. CLASSIFICATION OF SUBJECT MATTER

H01B 12/02(2006.01)i, H01B 1/04(2006.01)i

According to International Patent Classification (IPC) or to both national classification and IPC

B. FIELDS SEARCHED

Minimum documentation searched (classification system followed by classification symbols)
H01B 12/02; H01L 29/00; C01G 55/00; H01L 39/12; B32B 5/00; C23C 16/32; C01B 31/02; B32B 3/10; B05D 3/10; C01B 31/04; C07C 25/00; H01B 1/04

Documentation searched other than minimum documentation to the extent that such documents are included in the fields searched
Korean utility models and applications for utility models
Japanese utility models and applications for utility models

Electronic data base consulted during the international search (name of data base and, where practicable, search terms used)
eKOMPASS(KIPO internal) & Keywords: graphene, superconductor, strain, doped

C. DOCUMENTS CONSIDERED TO BE RELEVANT

Category*	Citation of document, with indication, where appropriate, of the relevant passages	Relevant to claim No.
A	US 2011-0269629 A1 (FELICIANO GIUSTINO et al.) 03 November 2011 See abstract, paragraphs [0003],[0026]-[0074] and figures 1(a)-6.	1-56
A	US 2012-0156424 A1 (KUEI-HSIEN CHEN et al.) 21 June 2012 See abstract, paragraphs [0010]-[0015] and figures 1A-8B.	1-56
A	US 2012-0003438 A1 (BILL R. APPLETON et al.) 05 January 2012 See abstract, paragraphs [0013]-[0018] and figure 1.	1-56
A	WO 2011-139236 A1 (NATIONAL UNIVERSITY OF SINGAPORE et al.) 10 November 2011 See abstract, paragraphs [0018]-[0055] and figures 1-12A.	1-56
A	US 2012-0288433 A1 (PETER WERNER SUTTER et al.) 15 November 2012 See abstract, paragraphs [0015]-[0018],[0050]-0077] and figures 1A-11.	1-56

☐ Further documents are listed in the continuation of Box C. ☒ See patent family annex.

* Special categories of cited documents:
"A" document defining the general state of the art which is not considered to be of particular relevance
"E" earlier application or patent but published on or after the international filing date
"L" document which may throw doubts on priority claim(s) or which is cited to establish the publication date of another citation or other special reason (as specified)
"O" document referring to an oral disclosure, use, exhibition or other means
"P" document published prior to the international filing date but later than the priority date claimed
"T" later document published after the international filing date or priority date and not in conflict with the application but cited to understand the principle or theory underlying the invention
"X" document of particular relevance; the claimed invention cannot be considered novel or cannot be considered to involve an inventive step when the document is taken alone
"Y" document of particular relevance; the claimed invention cannot be considered to involve an inventive step when the document is combined with one or more other such documents,such combination being obvious to a person skilled in the art
"&" document member of the same patent family

Date of the actual completion of the international search	Date of mailing of the international search report
12 August 2014 (12.08.2014)	**12 August 2014 (12.08.2014)**

Name and mailing address of the ISA/KR

International Application Division
Korean Intellectual Property Office
189 Cheongsa-ro, Seo-gu, Daejeon Metropolitan City, 302-701, Republic of Korea
Facsimile No. +82-42-472-7140

Authorized officer

JEONG, Jae Heon
Telephone No. +82-42-481-5417

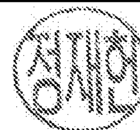

INTERNATIONAL SEARCH REPORT

Information on patent family members

International application No.

PCT/US2014/030887

Patent document cited in search report	Publication date	Patent family member(s)	Publication date
US 2011-0269629 A1	03/11/2011	GB 201004554 D0	05/05/2010
US 2012-0156424 A1	21/06/2012	TW 201223774 A	16/06/2012
US 2012-0003438 A1	05/01/2012	WO 2010-096646 A2	26/08/2010
		WO 2010-096646 A3	04/11/2010
WO 2011-139236 A1	10/11/2011	CN 103026490 A	03/04/2013
		EP 2567403 A1	13/03/2013
		JP 2013-537700 A	03/10/2013
		KR 10-2013-0098884 A	05/09/2013
		SG 184904 A1	29/11/2012
		US 2013-0048952 A1	28/02/2013
US 2012-0288433 A1	15/11/2012	US 8728433 B2	20/05/2014